

OPTIMISATION OF A SOLAR-POWERED HIGH ALTITUDE LONG ENDURANCE UAV

Olivier Montagnier , Laurent Bovet¹

**Flight Dynamics Team, Research centre of the French Air Force, Base Aérienne 701, 13661
Salon air, France**

Keywords: *HALE, solar powered, composite structure, optimisation*

Abstract

High altitude high endurance solar powered UAV can be a solution for many missions. The design complexity is due to the very high altitudes expected and the low available energy to supply the engines. During time of daylight, the solar energy is converted by photovoltaic cells and then used to supply electrical motors and payload. The energy remaining part is stored in a regenerative fuel cell and in potential energy with a climb maneuver. At night, fuel cell provides energy necessary to motors and payload. Optimisation carried out here consists in maximising the payload for a fixed total mass. It requires mass model for each constitutive part of the aircraft. In particular, the mass of the wing is minimised by the use of composite materials and by tolerate a large flexibility. An new analytical mass model is proposed here very useful for this particular application. Optimisation shows the existence of the UAV in a cruise speed versus lift coefficient diagram. This one revealed an optimal solution having a payload of about 4 % of the total mass of 817 kg for a 69 m wing span.

1 Introduction

Solar-powered HALE (High Altitude High Endurance) UAV could be a complement for many scientific missions like earth monitoring (early forest fire mapping, flood control, hurricane tracking and agriculture remote sensing [1]), an alternative for surveillance mission (security and

border controls) and a substitute for telecommunication satellites (operates in stationary orbits or at great range, low cost platform, low cost maintenance, ...). For this kind of operation, these UAVs should have the capabilities to flight over the civil transport traffic at least weeks to months. Since the 90s, several works were carried out on the design of these UAVs [2, 3, 4, 5]. The NASA ERAST program (Environmental Research Aircraft and Sensor Technology) was the main project on these problematics. The NASA showed the possibilities of solar-powered HALE UAVs with several platforms like "Pathfinder Plus" prototype which has reached an altitude of 24 km [6] but this success was mared by the crash of the "Helios" prototype [7].

Design difficulty are due to the very high altitude expected (more than 20 km) and the low available energy. During time of daylight, the solar energy is converted by photovoltaic cells and then used to supply electric motors and payload. The energy remaining part is stored in a regenerative fuel cell and in potential energy with a climb maneuver. At night, fuel cell provides energy necessary to motors and payload.

Air density at 20 km comparatively to 0 km is ten times lower. Therefore, wing surface must be very large. Feasibility can be obtain by decreasing dramatically structural mass of the aircraft. Firstly, wing mass can be reduced using composite materials and tolerating high flexibility. Secondly, aircraft mass can be reduced by suppressing lifting and control surfaces like tail, for example, by using electric motors to control yaw and stable aerofoil. Fig. 1 shows an artist view of the solar-powered HALE UAV considered here.

Margins are very small. Optimised UAV

¹New address : Airbus France, 316 route de Bayonne, 31060 Toulouse cedex 03, France.



Fig. 1 Artist view of the solar-powered HALE UAV

should be obtained with multidisciplinary optimisation tools (MDO). The aim of this work is to compute optimal parameters of a UAV with straight wings for a fixed wing aspect ratio and a fixed mass. Unlike classical design approach, size and cruise speed are the optimised parameters to maximise payload. Mass models, which are critical points of this kind of optimisation, are considered accurately. In particular, a composite wing mass model is proposed. Wing technology consists of a tubular beam with hybrid carbon/epoxy plies and constant cross section. This analytical model is well adapted to a wide range of solar-powered HALE UAV with straight wings.

2 Atmospheric and solar radiance

Design of a Solar-powered HALE need to take account of wind, solar radiation and atmosphere.

Main mission of this aircraft will consist in stationary flight. Therefore, cruise speed must be higher than air speed in the flight area. A study of Romeo *et al.* [4] shows wind speed in Italy is twice as much lower at 20 km than at 10 km, maximum gust and average wind are equal to 40 m.s^{-1} and 26 m.s^{-1} , respectively. These values are taken as a reference.

The solar radiance model gives the power used by the photovoltaic cells per unit area \bar{P}_s . Only normal part of solar radiance is transformed by the cells, the other part is reflected. This radiance power is a function of aircraft altitude h , of aircraft latitude ϕ , of day of the year \hat{d} and solar time \hat{h} , which can be written in the following form [8] :

$$\bar{P}_s = \frac{G_{SC}}{d^2} A_s \left(\sin \delta \sin \phi + \cos \delta \cos \phi \cos \frac{\pi \hat{h}}{12} \right) \quad (1)$$

$$d^2 = \left(1 + 0.033 \cos \frac{2\pi \hat{d}}{365} \right)^{-1}$$

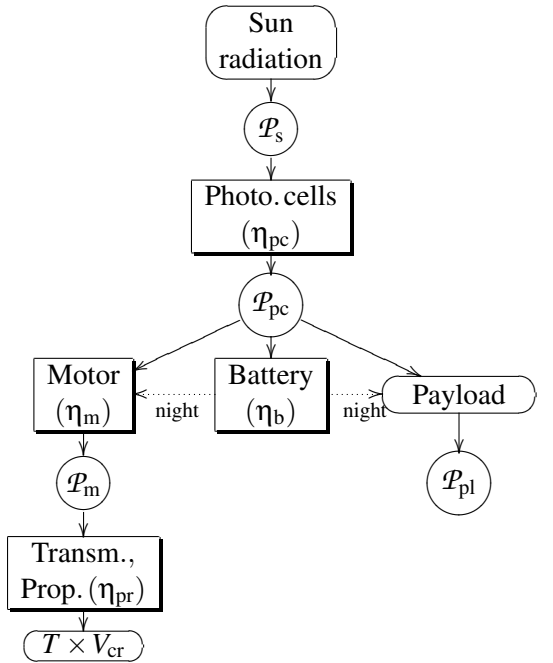


Fig. 2 Block diagram of power distribution

$$\begin{aligned} \phi &= 23.45 \sin \left(\frac{2\pi (284 + \hat{d})}{365} \right) \\ A_S &= \frac{1}{2} (e^{-0.65\Pi} + e^{-0.095\Pi}) \\ \Pi &= \frac{p}{p_0} (\sqrt{1229 + (614 \cos(\phi - \delta))^2} - 614 \cos(\phi - \delta)) \end{aligned}$$

where G_{SC} is the solar constant ($\approx 1374 \text{ W.m}^{-2}$), A_S the alleviation coefficient of solar radiant flux through the atmosphere, d the relative earth–sun distance in astronomical units, p the static pressure at altitude considered and p_0 the static pressure on the ground.

3 Aircraft modelling

3.1 Energy and power distribution

The aircraft uses only the solar irradiance. This energy is converted to electrical energy by photovoltaic cells and then distributed to the electrical motors, the payload and the battery (Fig. 2). At night, the aircraft flies only with energy stored in the battery. To decrease the mass of the battery it is possible to store extra daytime solar energy in potential energy by a climb maneuver (Fig. 3). The descent during night is realised with reduced motor power comparatively to cruising power.

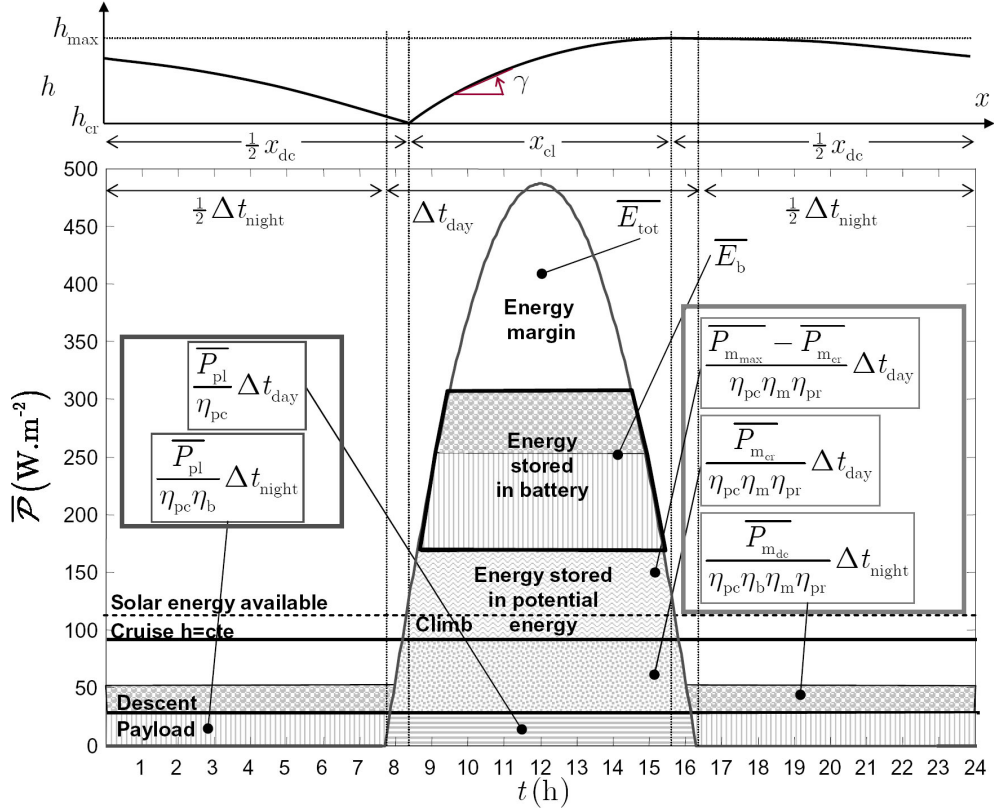


Fig. 3 Solar irradiance per unit area available vs time and distribution of energy to motors, battery and payload, and altitude vs position (22th of December at 45° of latitude and 18km of altitude)

3.1.1 Electric motor

The mass of electric motors is defined by the maximum useful power for the climb maneuver $\mathcal{P}_{m_{\max}}$. This power is assumed to be proportional to the cruise power

$$\mathcal{P}_{m_{\max}} = \xi_{\mathcal{P}_{m_{\max}}} \mathcal{P}_{m_{cr}} \quad (2)$$

$$\mathcal{P}_{m_{cr}} = \frac{T_{cr} V_{cr}}{\eta_{pr}} = \frac{mg V_{cr}}{\eta_{pr} f_{cr}} \quad (3)$$

where V_{cr} , T_{cr} , η_{pr} , f_{cr} , m and $\xi_{\mathcal{P}_{m_{\max}}}$ are the cruising velocity, the cruising thrust, the propeller efficiency, the cruising lift to drag ratio, the mass of the aircraft and the propeller efficiency, respectively. For a specific motor mass \bar{m}_m , the mass of motors can be written in the following form

$$m_m = \bar{m}_m \frac{\xi_{\mathcal{P}_{m_{\max}}} mg V_{cr}}{\eta_{pr} f_{cr}} \quad (4)$$

3.1.2 Climb and descent maneuver

The objective of the climb and descent maneuver is the storage of potential energy to reduce

size of Energy storage system (ESS). Examples of optimisation of these maneuvers are proposed in [2, 5]. The first maneuver consists in an UAV climb from cruise altitude to maximal altitude with maximum power available. The second phase corresponds to the descent during the night with reduced power. Here, these two phases are controlled assuming the term ρV^2 ($= \rho_{cr} V_{cr}^2$) to be constant. This choice gives a constant lift to drag ratio. Then linearised equation of motion is

$$\gamma = \frac{T}{mg} - \frac{1}{f_{cr}} = \underbrace{\frac{\eta_{pr} \mathcal{P}_m}{mg V_{cr} \sqrt{\rho_{cr}}}}_A \sqrt{\rho} - \frac{1}{f_{cr}} \quad (5)$$

with $\mathcal{P}_m = \mathcal{P}_{m_{\max}}$ for climb and $\mathcal{P}_m = \mathcal{P}_{m_{dc}}$ for descent where γ is the aircraft slope and ρ is the air density. To simplify the integration of Eq. (5), we assume square root of the air density linearly relative to the altitude in the range considered

$$\sqrt{\rho} = \underbrace{\frac{\sqrt{\rho_2} - \sqrt{\rho_1}}{h_2 - h_1} h + \frac{h_2 \sqrt{\rho_1} - h_1 \sqrt{\rho_2}}{h_2 - h_1}}_b \quad (6)$$

where ρ_i is computed at altitude h_i with U.S. Standard Atmosphere. This approximation is sufficiently accurate for a preliminary design ($\Delta\rho/\rho < 7\%$ in the range 18km to 24km). Then for the climb maneuver, the altitude can be obtained in a analytical form

$$h = (h_{\text{cr}} - h_{\text{ce}_{\text{cl}}}) e^{A_{\text{cl}} a x} + h_{\text{ce}_{\text{cl}}} \quad (7)$$

where $h_{\text{ce}_{\text{cl}}} = \frac{1}{A_{\text{cl}} a f_{\text{cr}}} - \frac{b}{a}$ and h_{cr} are the ceiling and cruising altitude, respectively. Inverse of previous equation gives the distance covered by the aircraft during climb

$$x_{\text{cl}} = \frac{1}{A_{\text{cl}} a} \ln \left(\frac{h_{\text{max}} - h_{\text{ce}_{\text{cl}}}}{h_{\text{cr}} - h_{\text{ce}_{\text{cl}}}} \right) \quad (8)$$

The duration of climb from cruise to maximal altitude (t_{cl}) can be computed with the following expression

$$\frac{dx}{dt} = V \Rightarrow \int_0^{x_{\text{cl}}} \frac{\sqrt{\rho}}{V_{\text{cr}} \sqrt{\rho_{\text{cr}}}} dx = \int_0^{t_{\text{cl}}} dt \quad (9)$$

and after some calculation

$$t_{\text{cl}} = \frac{1}{V_{\text{cr}} \sqrt{\rho_{\text{cr}}}} \left(\frac{h_{\text{cr}} - h_{\text{ce}_{\text{cl}}}}{A_{\text{cl}}} (e^{A_{\text{cl}} a x_{\text{cl}}} - 1) + (ah_{\text{ce}_{\text{cl}}} + b)x_{\text{cl}} \right) \quad (10)$$

As we considered $t_{\text{cl}} = \Delta t_{\text{day}} = t_{\text{ss}} - t_{\text{sr}}$ (where t_{sr} and t_{ss} are the sunrise time and sunset time, respectively), it is possible to obtain h_{max} with combination of Eqs. (8) and (10)

$$h_{\text{max}} + \frac{1}{A_{\text{cl}} a f_{\text{cr}}} \ln(h_{\text{max}} - h_{\text{ce}_{\text{cl}}}) = F_{\text{cl}} \quad (11)$$

with $F_{\text{cl}} = A_{\text{cl}} V_{\text{cr}} \sqrt{\rho_{\text{cr}}} \Delta t_{\text{day}} + h_{\text{cr}} + \frac{1}{A_{\text{cl}} a f_{\text{cr}}} \ln(h_{\text{cr}} - h_{\text{ce}_{\text{cl}}})$. The real root of the Eq. (11) is obtained numerically.

The same equations are obtained for the descent maneuver. In this case, the problem is to find $\mathcal{P}_{\text{m}_{\text{dc}}}$ for a duration of descent from maximal to cruise altitude of Δt_{night} . The distance covered by the aircraft during descent is

$$x_{\text{dc}} = \frac{1}{A_{\text{dc}} a} \ln \left(\frac{h_{\text{cr}} - h_{\text{ce}_{\text{dc}}}}{h_{\text{max}} - h_{\text{ce}_{\text{dc}}}} \right) \quad (12)$$

with $h_{\text{ce}_{\text{dc}}} = \frac{1}{A_{\text{dc}} a f_{\text{cr}}} - \frac{b}{a}$. The duration of descent is

$$\Delta t_{\text{night}} = \frac{1}{V_{\text{cr}} \sqrt{\rho_{\text{cr}}}} \left(\frac{h_{\text{cr}} - h_{\text{ce}_{\text{dc}}}}{A_{\text{dc}}} (e^{A_{\text{dc}} a x_{\text{dc}}} - 1) + (ah_{\text{ce}_{\text{dc}}} + b)x_{\text{dc}} \right) \quad (13)$$

Eqs. (12) and (13) can be combined to obtain the motor power for the climb maneuver

$$\mathcal{P}_{\text{m}_{\text{dc}}}^2 - \frac{mg(h_{\text{cr}} - h_{\text{max}})}{\eta_{\text{pr}} \Delta t_{\text{night}}} \mathcal{P}_{\text{m}_{\text{dc}}} - \mathcal{P}_{\text{m}_{\text{cr}}} \times \frac{mg \sqrt{\rho_{\text{cr}}}}{\eta_{\text{pr}} a \Delta t_{\text{night}}} \ln \left(\frac{\mathcal{P}_{\text{m}_{\text{dc}}} - \mathcal{P}_{\text{m}_{\text{cr}}}}{\sqrt{\frac{\rho_{\text{max}}}{\rho_{\text{cr}}}} \mathcal{P}_{\text{m}_{\text{dc}}} - \mathcal{P}_{\text{m}_{\text{cr}}}} \right) = 0 \quad (14)$$

The real root of this equation is obtained numerically.

It is then possible to compute an efficiency for these two maneuvers comparatively to a constant altitude flight

$$\eta_{\text{cl}/\text{dc}} = \frac{(\Delta t_{\text{day}} + \Delta t_{\text{night}}) \mathcal{P}_{\text{m}_{\text{cr}}}}{\Delta t_{\text{day}} \mathcal{P}_{\text{m}_{\text{max}}} + \Delta t_{\text{night}} \mathcal{P}_{\text{m}_{\text{dc}}}} \quad (15)$$

3.1.3 Photovoltaic cells

The solar radiance power per unit area $\bar{\mathcal{P}}_s$ is transformed in electric power $\bar{\mathcal{P}}_{\text{pc}}$ by the solar cells with an efficiency η_{pc} . Then, electric power is consumed by payload (\mathcal{P}_{pl}), battery (\mathcal{P}_{b}) with an efficiency η_{b} and electric motor power during climb maneuver ($\mathcal{P}_{\text{m}_{\text{max}}}$) with an efficiency η_{m} . At midday, we have

$$\mathcal{P}_{\text{pc}} \approx \frac{\mathcal{P}_{\text{m}_{\text{max}}}}{\eta_{\text{m}}} + \mathcal{P}_{\text{pl}} + \frac{\mathcal{P}_{\text{b}}}{\eta_{\text{b}}} = \eta_{\text{pc}} \bar{\mathcal{P}}_{\text{smax}} S_{\text{pc}} \quad (16)$$

where S_{pc} is the solar cells surface. Thus, using Eqs. (2) and (3), we can obtain the mass of the cells

$$m_{\text{pc}} = \frac{\tilde{\rho}_{\text{pc}}}{\eta_{\text{pc}} \bar{\mathcal{P}}_{\text{smax}}} \left(\frac{\xi_{\mathcal{P}_{\text{m}_{\text{max}}}}}{\eta_{\text{pr}} \eta_{\text{m}}} \frac{mg V_{\text{cr}}}{f_{\text{cr}}} + \mathcal{P}_{\text{pl}} + \frac{\mathcal{P}_{\text{b}}}{\eta_{\text{b}}} \right) \quad (17)$$

where $\tilde{\rho}_{\text{pc}} = m_{\text{pc}} / S_{\text{pc}}$ is the cell surface density.

3.1.4 Fuel cell

Various studies show that regenerative fuel cell, including pressure vessels for H₂ and O₂, tank

for H_2O and other systems, has a very high specific energy. This ESS size and mass depends only on the energy necessary for the night flight. Energy stored E_{ESS} is used to supply motors during descent maneuver and payload

$$E_{ESS} = \Delta t_{night} \left(\frac{P_{m_{dc}}}{\eta_m} + P_{pl} \right) \quad (18)$$

Mass of ESS can be then computed with the specific energy $\widehat{E}_{ESS} = E_{ESS}/m_{ESS}$.

3.2 Drag model

Total drag coefficient C_D is the sum of zero-lift drag coefficient C_{D0} and induced drag :

$$C_D = C_{D0} + \frac{1}{\pi \lambda} C_L^2$$

where $\lambda = b/c$, C_L , b and c are the wing aspect ratio, the lift coefficient, the wingspan and the aerofoil chord, respectively. The drag coefficient without lift is assumed to be equal to the sum of drag due to the aerofoil form and those of the body. Models are elaborate in [9].

3.3 Wing mass

3.3.1 Wing design

Models used in the optimisation problem need to have a physical sense for a wide range of solar-powered HALE UAVs. In particular, the wing mass model needs to have a technological sense for a wide range of wing surfaces. In other word, this model must be generic. The wing architecture proposed is a “tubular structure” (Fig. 4). The wing with rectangular form is constituted of :

- a tubular beam with non-constant cross sections and constant composite laminate stacking sequence. At the wing-root, inner and outer radius are r_{i0} and r_{o0} , respectively. The wing-root outer radius is defined by the expression $r_{o0} = \varepsilon_r \varepsilon_e l / 2$ where $\varepsilon_r < 1$, e and $\varepsilon_e = e/l$ are the relative diameter of the beam, the aerofoil thickness and the relative aerofoil thickness, respectively. The parameter κ characterised the linear variation of radius along the wing i.e. $r_o(y) = r_{o0} (1 - \kappa \frac{y}{b})$ with $\kappa \in [0, 1]$, $y \in [0, b/2]$;

- ultra-light ribs in composite materials (for example, made with RTM process), their total mass is $m_{rib} \approx n_{rib} \varpi_{rib} l / 2$ where $n_{rib} = E(2b)$ is the number of ribs (E is the entier function) and ϖ_{rib} is the mass of the rib per unit area ;
- ultra-light skins, their total mass is $m_{skin} \approx \varpi_{skin} b (2l + e)$ where ϖ_{skin} is the mass of the skin per unit area ;
- secondary parts like components of hinged surfaces, local reinforcements, small tubular beam to rigidify the trailing edge of the wing, ... their total mass is $m_{remw} = \xi_{remw} m_w$ where m_w and $\xi_{remw} < 1$ are the mass of the wings and the percentage of mass of the secondary parts in the wing, respectively.

Main beam is assumed to be the only part that bear aerodynamic and inertial forces. If beam was constituted of homogeneous material like aluminium, the optimisation would be only the computation of geometric parameters [10]. Nevertheless, the specific modulus (Young's modulus/density) of homogeneous materials is not enough large to obtain a lightweight structure. In modern aircraft structures, carbon/epoxy laminates are preferred because specific modulus can be five times larger. This material is chosen for the beam. In this case, the optimisation is more complex and choices should be made like parameters of the stacking sequence, carbon fibres, parameters of the beam, ... These choices are not necessary if an optimisation algorithm of the stacking sequence is used like a genetic algorithm well adapted for the stacking sequence search [11].

Here, we choose a generic stacking sequence well adapted to bending and torsion problems: $[0^\circ_{n_0}, \pm 45^\circ_{n_{\pm 45}}]$ where n_0 and $n_{\pm 45}$ are the unknown number of 0° and $\pm 45^\circ$ plies, respectively (Fig. ??). This laminate has the advantage to approximately uncouple the flexural resistance problem and torsional resistance problem. It is well known that 0° plies are the stiffness and strength optimum for a composite beam in bending as well as $\pm 45^\circ$ plies are the stiffness and strength optimum for a composite beam in torsion. If 0° plies and $\pm 45^\circ$ plies are consti-

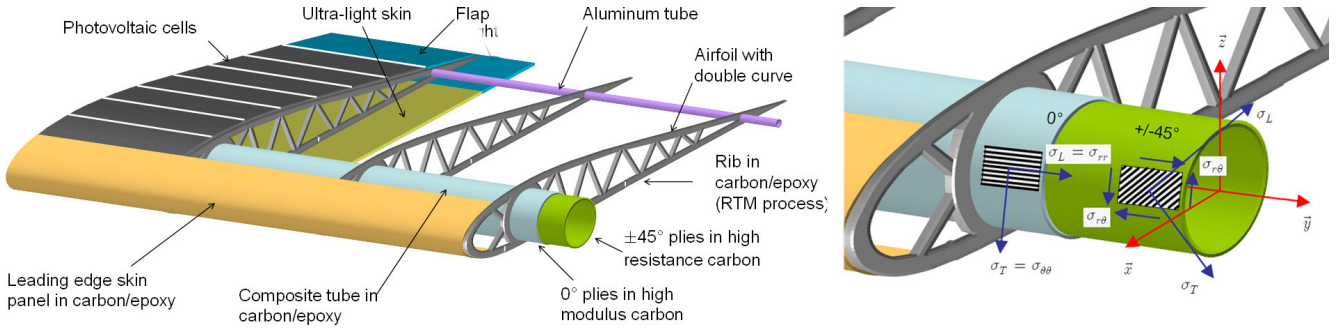


Fig. 4 Sketch of the wing configuration called “tubular structure” and laminates orientations

tuted of various fibres with the same epoxy resin, the composite material is called *hybrid carbon/epoxy material*. For example, high modulus carbon fibres used for 0° plies can increase widely the flexural wing stiffness. High resistance carbon fibres used for 0° plies can increase the wing strength in tension and compression.

The aim of the wing optimisation is to minimise the total number of plies (n_0 and $n_{\pm 45}$) and to maximise the parameter κ to minimise the mass of the main beams. If $\kappa = 0$, the mass is $m_{beam0} = \rho_0 \pi b (r_{o0}^2 - r_{f0}^2) + \rho_{\pm 45} \pi b (r_{f0}^2 - r_{i0}^2)$ where ρ_i is the mass density of the ply i and r_{f0} is the boundary radius of the beam between 0° and $\pm 45^\circ$ plies. If $\kappa \in]0, 1]$ and $\frac{t}{r_{o0}} = 1 - \frac{r_{i0}}{r_{o0}} \ll 1$, the mass of the beam is $m_{beam} \approx \frac{2-\kappa}{2} m_{beam0}$ where t is the thickness of the beam.

3.3.2 Wing resistance

To simplify dramatically the modelling and minimise dynamical coupling effects between bending and torsion, the centre of gravity of a wing section is assumed to be located at the centre of the beam cross section which is located at the aerodynamic centre of the aerofoil (approximately quarter-chord point).

The forces acting on a wing section are composed of aerodynamic forces and inertial forces. The first can be decomposed in two parts, one part provided by the aerofoil and the second one provided by the position of ailerons. The general case of sizing loads, i.e. CS22 adapted to HALE UAVs, is presented in [12]. A simplified formulation is proposed in [13] to obtain an analytical wing mass model with several assumptions: same aerofoil for all sections ; rectangular wing ; lifting and moment coefficient of the wing equal

to that of the aerofoil ; lift provided only by the wing. The first loading case is design at extreme load factor (turning flight stall). The second loading case is design aileron down limit speed.

We work with the beam theory and material is assumed to be elastic linear. The small thickness of the tubular beam comparatively to the radius allows us to assume a plane stress field in the skin of the tube. Therefore, we can work with a simplified laminate theory which assume that coupling effect between 0° and $\pm 45^\circ$ plies is negligible. It is clear that computation results need to be verified with the classical laminate theory [14] after optimisation.

With these important assumptions, we write the maximum/minimum stress in the 0° plies at the root of the wing due to first loading case:

$$\sigma_{max.0} = \frac{E_{yy0} r_{o0} b n_{ext} (m - m_w - m_m) g}{8(EI)_{yyhom}} = -\sigma_{min.0}$$

$$(EI)_{yyhom} \approx \pi r_{o0}^3 t_{ply} [n_0 E_{yy0} + 2n_{\pm 45} E_{yy\pm 45}]$$

where E_{yyi} is the tensile modulus in the y direction for the ply i (Fig. 4). We write the maximum stress in the $\pm 45^\circ$ plies at the root of the wing due to second loading case:

$$\begin{aligned} \sigma_{max.\pm 45} &= \frac{E_{yy\pm 45} r_{f0} b n_{asym} (m - m_w - m_m) g}{8(EI)_{yyhom}} \\ &= -\sigma_{min.\pm 45} \\ \tau_{max.\pm 45} &= \frac{E_{xy\pm 45} r_{f0} l n_{asym} m g}{2(EJ)_{xyhom}} \frac{C_{M_o} + \frac{b_a}{b} C_{M_{\delta_m}} \delta_m}{C_{L_{max}}} \end{aligned}$$

$$(EJ)_{xyhom} \approx 2\pi r_{o0}^3 t_{ply} [n_0 E_{xy0} + 2n_{\pm 45} E_{xy\pm 45}]$$

where E_{xyi} is the shear modulus in the xy direction for the ply i and b_a is the total length of the ailerons.

For the UAV optimisation, the strength computation must be as simple as possible. Strain or a stress criterion are well adapted. Here, we work with the Tsai-Wu criterion [14] which can be written in the ply coordinate system

$$\frac{\sigma_L^2}{XX'} - \frac{\sigma_L\sigma_T}{\sqrt{XX'YY'}} + \frac{\sigma_T^2}{YY'} + \frac{\sigma_{LT}^2}{C^2} + \left(\frac{1}{X} - \frac{1}{X'} \right) \sigma_L + \left(\frac{1}{Y} - \frac{1}{Y'} \right) \sigma_T = 1 \quad (19)$$

where L , T and LT signify longitudinal, transverse and in-plane shear ; X , X' , Y , Y' and C are maximal strength in longitudinal tension, in longitudinal compression, in transverse tension, in transverse compression and in in-plane shear, respectively.

For the first loading case and for the 0° plies, local stress are: $\sigma_L = \sigma_{yy}$, $\sigma_T = \sigma_{\theta\theta} = 0$ and $\sigma_{LT} = \sigma_{y\theta} = 0$. Therefore, Tsai-Wu criterion is written in the following form

$$(\sigma_{yy} - X)(\sigma_{yy} + X') = 0 \quad (20)$$

Classically in carbon/epoxy materials, the longitudinal strength in tension is higher than in compression $X \geqslant X'$ then criterion can simply rewrite in a constraint form

$$\sigma_{\max,0} \leqslant X' \quad (21)$$

In the case of this simplified approach, it can be assumed that fibre fracture in the 0° plies happen before the fracture in the $\pm 45^\circ$ plies, because maximal strain of 0° plies is lower than $\pm 45^\circ$ plies. This assumption is conservative.

For the second loading case and for the $\pm 45^\circ$ plies, it is necessary to write the criterion in the ply coordinate system that is computing shear stress in a coordinate system at 45° (or -45°) relatively to \vec{y} . This coordinate system rotation gives the following local stress: $\sigma_L = \frac{\sigma_{yy}}{2} + \sigma_{y\theta}$, $\sigma_T = \frac{\sigma_{yy}}{2} - \sigma_{y\theta}$ and $\sigma_{LT} = -\frac{\sigma_{yy}}{2}$. Therefore, Tsai-Wu criterion is written in the following form

$$\begin{aligned} & \frac{1}{4} \left(\frac{1}{XX'} - \frac{1}{\sqrt{XX'YY'}} + \frac{1}{YY'} + \frac{1}{C^2} \right) \sigma_{\max,\pm 45}^2 + \\ & \underbrace{\left(\frac{1}{XX'} + \frac{1}{\sqrt{XX'YY'}} + \frac{1}{YY'} \right)}_A \tau_{\max,\pm 45}^2 + \frac{1}{2} \left(\frac{1}{X} - \frac{1}{X'} + \frac{1}{Y} \right) \\ & - \frac{1}{Y'} \sigma_{\max,\pm 45} + \underbrace{\left(\frac{1}{X} - \frac{1}{X'} - \frac{1}{Y} + \frac{1}{Y'} \right)}_B \tau_{\max,\pm 45} = 1 \end{aligned} \quad (22)$$

In the case of this simplified approach, longitudinal stress in $\pm 45^\circ$ plies are neglected. Moreover, in carbon/epoxy materials, strength in transverse compression is higher than in tension i.e., $Y' \geqslant Y$. With previous $X \geqslant X'$ assumption, we have $A \geqslant 0$ and $B \leqslant 0$. Then, Tsai-Wu criterion can be written in the following form:

$$\tau_{\max,\pm 45} \leqslant \frac{B + \sqrt{B^2 + 4A}}{2A} = D \quad (23)$$

Finally, after some calculations and assuming $\frac{t}{r_{o_0}} \ll 1$ and $\kappa = 0$, the validation of Eqs. (21) and (23) can be rewritten in the following form that gives directly number of 0° plies and $\pm 45^\circ$ plies in an analytical form

$$n_{\pm 45} = \text{UpRd} \left(\frac{a_1 a_5 - a_4 a_3}{a_1 - a_2 a_4} \right) \quad (24)$$

$$n_0 = \text{UpRd} \left(\frac{a_3 - a_2 a_5}{a_1 - a_2 a_4} \right) \quad (25)$$

$$\begin{aligned} a_1 &= \frac{2r_{o_0}X'}{\rho_{\pm 45}b^2 n_{\text{extg}}} (1 - \xi_{remw}) + \frac{\rho_0}{2\rho_{\pm 45}} \\ a_2 &= \frac{4r_{o_0}X'}{\rho_{\pm 45}b^2 n_{\text{extg}}} \frac{E_{yy\pm 45}}{E_{yy_0}} (1 - \xi_{remw}) + 1 \\ a_3 &= \frac{(m - m_m)(1 - \xi_{remw}) - m_{\text{skin}} - m_{\text{rib}}}{4\pi b r_{e_0} t_{\text{ply}} \rho_{\pm 45}} \\ a_4 &= \frac{E_{xy_0}}{2E_{xy\pm 45}} \\ a_5 &= \frac{\ln_{tors} mg}{8\pi r_e^2 t_{\text{ply}} D} \frac{C_{M_o} + \frac{b_a}{b} C_{M_{\delta_m}} \delta_m}{C_{L_{2/3}}} \end{aligned}$$

where UpRd(.) is the upper round-off function.

Buckling risk in torsion is not taken into account in this paper. To avoid local buckling risk, a thickness constraint is set $t = r_e - r_i \leqslant t_{\min}$ where $t_{\min} = 1.5$ mm is the minimal thickness of the beam.

3.3.3 Wing flexibility

A wing which satisfies the strength criterion can be too largely flexible, which strongly deteriorate the aircraft performances. This phenomenon is as much more significant than the wing has a large aspect ratio. This deformation implies a lift

reduction and causes a parasitic drag. It is necessary to define a displacement criterion *i.e.*, a maximal displacement of the wing tip : $u_{z,\max} \leq \Lambda_{\max} \frac{b}{2}$ where Λ_{\max} is the relative maximal displacement. With Euler-Bernoulli assumption with a constant stacking sequence but linearly decreasing cross section, the displacement is written after some computations

$$u_{z,\max} = \frac{n_{extgb^3}}{128(EI)_{yyhom}} \left(4 \frac{m - m_m - m_{skin} - m_{rib}}{m_{beam0}} - 2 + \kappa \right) \frac{6(1-\kappa)\ln(1-\kappa) + 6\kappa - 3\kappa^2 - \kappa^3}{2\kappa^4} \quad (26)$$

Finally, the following criterion gives the parameter κ

$$\text{find } \kappa \in [0, 1] / u_{z,\max} - \Lambda_{\max} \frac{b}{2} = 0$$

3.4 Remaining structural mass

The mass of the fuselage is expressed with the Roskam model: $m_{fus} = 0.232 m^{0.95}$ [15]. Lastly, mass of the tail and the landing gear are supposed to be proportional to the total mass *i.e.*, $m_{tail} = \xi_{tail} m$ and $m_{gear} = \xi_{gear} m$. We note $m_{rem} = m_{fus} + m_{gear} + m_{tail}$.

4 Optimisation procedure

The total mass of the UAV is:

$$m = m_w + m_m + m_{pc} + m_b + m_{rem} + m_{pl} \quad (27)$$

where m_{pl} is the mass of the payload. This mass is the variable to maximise. Then, a merit function \mathcal{MF} to minimise can be obtained:

$$\frac{m_{pl}}{m} = 1 - \frac{m_w + m_m + m_{pc} + m_b + m_{rem}}{m} = 1 - \mathcal{MF} \quad (28)$$

It is clear that $m_{pl} > 0$ *i.e.*,

$$\mathcal{MF} \leq 1 \quad (29)$$

The second constraint is the solar cells total surface S_{pc} must be inferior to the wing surface

$$\frac{S_{pc}}{S_w} = \mathcal{T} \leq \mathcal{T}_{\max} \quad (30)$$

where \mathcal{T}_{\max} is the maximal occupancy rate. Previous study [13] shows that optimal UAV is obtained when maximal cell occupancy rate is reached.

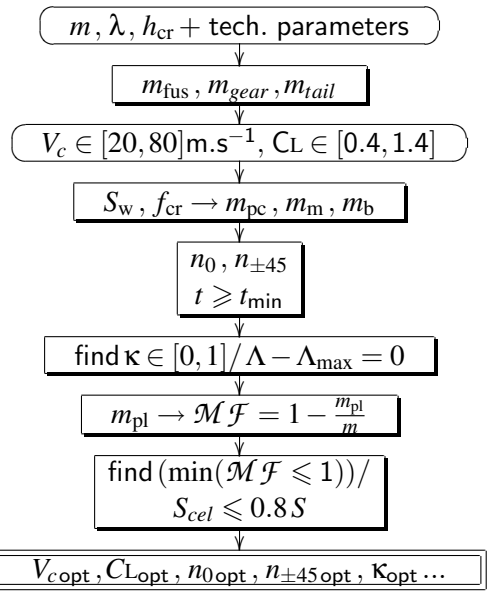


Fig. 5 Algorithm diagram to compute the optimised UAV

The third constraint is the energy consumption that must be inferior to the total available solar energy during one day

$$E_{\text{tot}} \leq \mathcal{E}_s = \int_{t_{sr}}^{t_{ss}} \overline{P}_s S_{pc} dt \quad (31)$$

where total energy consumption of the UAV during one day is given by

$$\begin{aligned} \mathcal{E}_{\text{tot}} = & \frac{1}{\eta_{pc}} \left(\Delta t_{\text{day}} \left(P_{pl} + \frac{P_{m_{max}}}{\eta_m} \right) \right. \\ & \left. + \frac{\Delta t_{\text{night}}}{\eta_b} \left(P_{pl} + \frac{P_{m_{dc}}}{\eta_m} \right) \right) \end{aligned} \quad (32)$$

The optimisation process corresponds to a Torenbeek method [16]. The maximum take-off weight and the endurance are fixed therefore the mass of payload has to be maximised (Fig. 5). The number of parameters is large and a selection is made to choose relevant conceptual parameters. The parameters scanned with the algorithm are the cruise speed V_{cr} and the lift coefficient CL which is directly proportional to the wing surface. The endurance is not under consideration because it is not a relevant parameter.

5 Case study

For this study, the wing aspect ratio λ and the maximum take-off weight m are fixed to 31.25 and

Table 1 UAV properties

\bar{m}_m	η_m	η_{pr}	η_{pc}	η_b	ϖ_{cel}	ϖ_{skin}
N.kW ⁻¹	-	-	-	-	kg.m ²	kg.m ²
32	0.96	0.92	0.183	0.50	0.45	0.1
ϖ_{ri}	ε_e	ε_r	Λ_{\max}	ξ_{remw}	ξ_{tail}	ξ_{gear}
kg.m ²	-	-	-	-	-	-
4.8	0.12	0.9	0.16	0.1	0	0.032
$\xi_{P_{m\max}}$	$C_{L\max}$	C_{M_o}	$C_{M_{\delta_m}}$	δ_m	n_{ext}	$\overline{\mathcal{E}_{ESS}}$
-	-	-	-	$^\circ$	-	Wh.kg ⁻¹
1.3	1.4	0.05	0.5	10	2	450

817 kg, respectively, which correspond to «Helios» prototype in fuel cell configuration. The cruise altitude h_{cr} is chosen equal to 60 000 ft. The latitude is 22° and the date is the 22th of June. The maximal occupancy rate of photovoltaic cells T_{\max} is 85 %. This value allows to distribute cells on the main part of the surface without the edges with high curvature. Other parameters of the UAV are given in Tabs. 1 and 2.

The contour of \mathcal{MF} and T_{\max} functions are plotted in the $(V_{cr}; CL)$ axes (Fig. 6). The constraint on the occupancy rate of photovoltaic cells decrease dramatically the feasibility domain. The merit function get a minimum called optimal point, approximately 0.9. The optimal point ($V_{opt} \approx 32 \text{ m.s}^{-1}$; $CL_{opt} \approx 0.89$) is on the $T = T_{\max}$ curve, which is not surprising. At this point, the mass of payload represents approximately 36 kg for a maximal take-off mass of 817 kg. The optimal velocity is over the maximum gusts. Other characteristics of the HALE are given in the Tab. 3.

6 conclusion

Optimisation carried out here consists in maximising the payload for a fixed total mass. It requires mass model for each constitutive part of the aircraft. In particular, the mass of the wing is minimised by the use of composite materials and by tolerate a large flexibility. An new analytical mass model is proposed here very useful for this particular application.

Optimisation shows the existence of the Solar-powered HALE UAV in a cruise speed versus lift coefficient diagram. This one revealed an optimal solution having a payload of about 4 % of the total mass of 817 kg for a 69 m wing span. No-

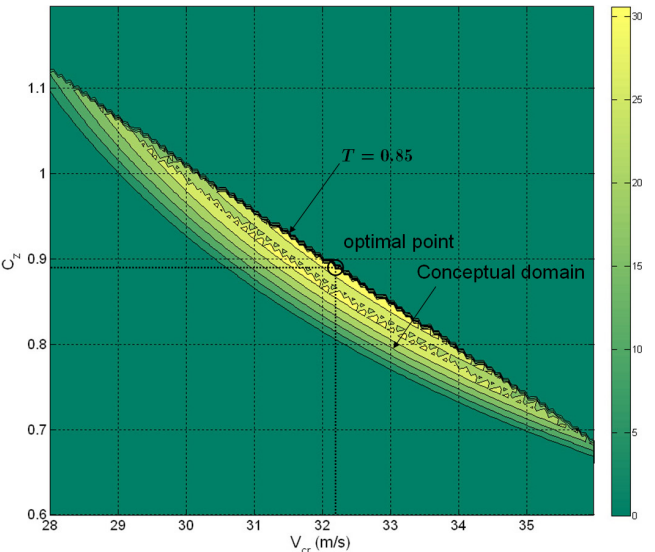


Fig. 6 Payload mass of the solar-powered HALE UAV in a cruise speed versus lift coefficient diagram

ting that computation is made with several pessimistic parameter values (low occupancy rate of photovoltaic cells, low efficiency of solar cells, high load factor) and several optimistic parameter values (day, hour).

This work needs to be continued to optimise the effect of wing aspect ratio. Then, the sizing during night operation in the aim to flight weeks to months will necessitate to add an energy storage system. Finally, an endurance computation will be realised.

7 Copyright Statement

The authors confirm that they, and/or their company or organization, hold copyright on all of the original material included in this paper. The authors also confirm that they have obtained permission, from the copyright holder of any third party material included in this paper, to publish it as part of their paper. The authors confirm that they give permission, or have obtained permission from the copyright holder of this paper, for the publication and distribution of this paper as part of the ICAS2010 proceedings or as individual off-prints from the proceedings.

References

- [1] S. R. Herwitz, L. F. Johnson, J. C. Arvesen, R. G. Higgins, J. G. Leung, S. E. Dunagan, Precision agriculture as a commercial application for solar-

Table 2 T800/M18 properties for a 0.6 volume fraction

ρ	$E_{11} = E_{yy0}$	E_{22}	$E_{66} \approx E_{xy0}$	E_{12}	$E_{yy\pm 45}$	$E_{xy\pm 45}$	X	X'	Y	Y'	S	t_{ply}
kg m^{-3}	GPa	GPa	GPa		GPa	GPa	MPa	MPa	MPa	MPa	MPa	mm
1 530	162	10	5.0	0.3	13.2	9.1	2 940	1 570	60	290	100	0.125

Table 3 Optimal UAV definition

S_w	b	l	W_S	m_w	m_m	m_{pc}	m_b	m_{rem}	m_{pl}	m_{beam}	m_{skin}	m_{rib}	m_{remw}	n_0	$n_{\pm 45}$
m^2	m	m	kg.m^2	kg	kg	kg	kg	kg	kg	kg	kg	kg	kg	-	-
151	68.9	2.2	5.42	385	43.6	57.6	133	162	35.7	120	32	194	39	2	9

powered unmanned aerial vehicles, in: 1st Unmanned Aerospace Vehicles, Systems, Technologies, and Operations Conference and Workshop, Portsmouth, VA, 2002.

- [2] M. Harmats, D. Weihs, Hybrid-propulsion high-altitude long-endurance remotely piloted vehicle, *Journal of Aircraft* 36 (2) (1999) 321–331.
- [3] B. Keidel, Design of a solar-powered hale aircraft for year-round operation at intermediate latitudes, in: Proceeding of the RTO symposium on “UV for aerial, ground and naval military operations”, Ankara, Turkey, 2000.
- [4] G. Romeo, G. Frulla, E. Cestino, G. Corsino, Heiliplat: Design, aerodynamic and structural analysis of very-long endurance solar powered stratospheric uav, *Journal of Aircraft* 41 (6) (2004) 1505–1520.
- [5] S. V. Serokhvostov, T. E. Churkina, Optimal control for the sunpowered airplane in a multi-day mission, in: 2nd European Conference for Aerospace Sciences (EUCASS), Brussels, Belgium, 2007.
- [6] K. Flittie, B. Curtin, Pathfinder solar-powered aircraft flight performance, in: Proceeding of the AIAA Atmospheric Flight Mechanics Conference & Exhibit, Boston, 1998.
- [7] T. Noll, J. Brown, M. Perez-Davis, S. Ishmael, G. Tiffany, M. Gaier, N. Headquarters, Investigation of the helios prototype aircraft mishap: Volume i mishap report, nasa, Tech. rep. (2004).
- [8] J. A. Duffie, W. A. Beckman, Solar engineering of thermal processes, John Wiley & Sons, Inc.
- [9] L. Bovet, Optimisation conceptuelle de la croisière - application aux avions de transport civils, Ph.D. thesis, University of Marseille, France (2004).
- [10] L. Bovet, O. Montagnier, Optimisation conceptuelle d'un drone à énergie solaire, Tech. rep., CReA (2006).
- [11] O. Montagnier, C. Hochard, Optimization of supercritical carbon/epoxy drive shafts using a genetic algoritm, in: Proceedings of the 13th

European Conference on Composite Materials, Stockholm, Sweden, 2008.

- [12] J. Raska, Pertinence des modèles de conception d'un avant-projet d'avion – application aux gnoptères hale, Ph.D. thesis, ENSAE (2000).
- [13] O. Montagnier, L. Bovet, Optimisation of a solar-powered high altitude long endurance uav with composite wings, in: Proceedings of the 3rd EUropean Conference for AeroSpace Sciences, Grenoble, France, 2007.
- [14] S. W. Tsai, E. M. Wu, A general theory of strength of anisotropic materials, *Journal of Composite Materials* 5 (1971) 58–69.
- [15] J. Roskam, Airplane Flight Dynamics and Automatic Flight Controls, Darcorporation, 2001.
- [16] E. Torenbeek, Synthesis of subsonic airplane design, Delft University Press, 1988.